

# ZnO nanostructured photocatalysts for water treatment applications

Magdy Lučić Lavčević\* and A. Penava

University of Split, Faculty of Chemistry and Technology, Ruđera Boškovića 35, 21000 Split, Croatia

original scientific paper

DOI: 10.17508/CJFST.2017.9.2.17

## Summary

Metal oxide semiconductor materials, designed to be applied in photocatalytic systems for water purification, are required to have large specific surface areas, because chemical reactions induced by suitable irradiation take place by contact between their surface and fluid. Zinc oxide is well known as a material that forms various morphologies at the micro- and nanoscale, which can easily fulfill this requirement in the case of ultraviolet irradiation. However, some nanoscaled morphologies can also provide zinc oxide catalysts that are functional in the sunlight. Photocatalytic degradation of an organic dye, as a model pollutant, was studied in aqueous solutions using structures of zinc oxide synthesized in the form of prism, spiky stick and grass blade. They were grown from a solution and their entire morphology was simply controlled by varying the growth conditions. Detailed characterization of their structure and porosity on the micro- and nanoscale was performed by scanning electron microscope and X-ray diffraction and scattering measurements. All structures exhibited notable photocatalytic activities. However, remarkable results were achieved with nanostructures in the form of grass blade, which exhibited enhanced photocatalytic activity in sunlike light. This was ascribed to their specific morphology characterized with defects and a high degree of mesoporosity.

**Keywords:** ZnO, nanostructures, mesoporosity, photocatalyst

## Introduction

The fast development of technologies and materials for purifying water from pollutants is present over a long period of time. One of the main objectives is getting the treatment that does not have a great impact on the environment and is not too expensive. Photocatalysis has the potential to fulfil this request, providing a relatively simple and low cost solution (Serpone et al., 1989). This is commonly considered as a chemical process, catalysed by a solid, and induced by suitable external radiation with wavelengths in the ultraviolet, visible or infrared range of the electromagnetic spectrum. Materials, designed to be applied in photocatalytic systems, are required to have large specific surface areas, because involved chemical reactions take place by contact between material and fluid. Using the sun as a source of radiation for water treatment requires a material that is functional in a broad range of wavelengths.

Photocatalysts are usually photostable and nontoxic semiconductors which are able to absorb ultraviolet and/or visible light. The most frequently used semiconductors are TiO<sub>2</sub>, ZnO, CeO<sub>2</sub>, WO<sub>3</sub>, Fe<sub>2</sub>O<sub>3</sub>, GaN, CdS and ZnS (Thompson et al., 2006). They are used as powders of particles, or in forms that can be spread on a substrate.

Due to their unique morphology and properties, nanostructured photocatalysts represent a step

forward the further improvement of the efficiency in photodegradation of water pollutants. Nanostructured materials have a particle size, phase (crystallite) or a thickness of the order of atomic level (about 0.1 nm) up to a few hundred nanometers. They have unique and more prominent characteristics compared to the same materials without nanoscaled features. Therefore, the physical and chemical properties of nanomaterials may differ from those inherent to the more massive substances or larger particles, i.e. to the substances with micro- and macroscale features. Properties and arrangement of the nanoscaled elements in nanomaterials determine the behaviour of such materials. The nanostructured semiconducting metal oxides can take a variety of forms including nanoparticles, nanorods, nanowires, nanotubes, nanosheets, nanoflowers, etc. A surface-to-volume ratio in nanostructured materials offers more active sites for reactions. The size reduction leads to novel surface and quantum effect (Colon et al., 2007).

ZnO is well known as semiconducting material that can be synthesized in various morphologies at the micro- and nanoscale (Kumari et al., 2010). It is an environmental friendly material, compatible with living organisms. The use of ZnO in nanoscale can alter its electrical, optical and magnetic properties. As a photocatalyst, it has limited absorption of radiation in the visible range, because of its wide band gap of around 3.26 eV. So, for the economic

\*Corresponding author: malula@ktf-split.hr

use in photocatalytic systems using sunlight, its optical properties should be modified by structuring or doping. Nanostructured ZnO is capable of operating effectively for water treatment via various nanotechnology routes (Baruah et al., 2012). Various morphologies of ZnO can be realized through different approaches of preparation. In this paper ZnO is prepared in three forms with different morphology, using relatively simple chemical synthesis. Not only the surface area, but also all other morphological elements (such as size, shape, crystallographic structure and porosity) have the influence on the photocatalytic activity, as it correlates with oxygen related defect states. The comprehensive description of detailed morphology on the micro- and nanoscale is important in the analysis of the functionality of the material.

## Materials and methods

For the present study, ZnO structures are precipitated by chemical synthesis from an aqueous solution at an elevated temperature, so-called hydrothermal deposition (Baruah et al., 2009). Field-emission scanning electron microscopy (FESEM), X-ray diffraction (XRD) measurements and small-angle X-ray scattering (SAXS), performed by using synchrotron radiation were used to characterize the three different samples of ZnO structures.

### *Preparation of ZnO structures*

By varying the conditions of preparation, such as temperature, concentration of precursors and time of growth, we can influence the overall morphology of ZnO structures. In this study, we used the effect of the concentration of precursors. Other preparation conditions, selected following the theoretical considerations and preliminary experiments, were kept constant.

The solution with precursors is prepared by mixing  $\text{Zn}(\text{NO}_3)_2 \cdot 6\text{H}_2\text{O}$  and  $\text{C}_6\text{H}_{12}\text{N}_4$ , at a constant volume ratio. All the chemicals were of analytical grade and used without further purification. Aqueous solutions were prepared using double distilled water. The reaction took place in closed containers, at elevated temperature (358 K) for 12 h. The precipitated powder with ZnO structures was washed several times with distilled water in order to remove residual salts and amino complexes. Finally, it was dried in air at 313 K. Three samples of ZnO structures were obtained using selected

concentrations of precursors: one from a 0.1 M solution, one from a 0.01 M solution, and one from a 0.001M solution.

### *Characterization of ZnO nanostructures*

The insight in general morphologies of the synthesized films was obtained in real space, by field emission scanning electron microscopy (FE-SEM Jeol 7000F). The analysis of crystallites in ZnO samples is based on the XRD measurements and mesoporosity of structures was estimated by an analysis in reciprocal space using SAXS method. Both, XRD and SAXS experiments were performed at the SAXS beamline at the Synchrotron Elettra in Italy (Amenitsch et al., 1995; Lavčević et al., 2002). A photon energy of 8 keV ( $\lambda = 0.155$  nm) was used. The XRD measurements were performed using a position sensitive detector, which covered an angular range ( $2\theta$ ) from  $20^\circ$  to  $50^\circ$ . Phase identification was realized matching diffracted peaks with crystallographic cards (PDF). The SAXS measurements were performed using two-dimensional CCD detector. The XRD and SAXS patterns were corrected for readout noise and detector response.

### *The photocatalytic activity test*

Photocatalytic experiments were performed in an open reactor with ZnO structures in the aqueous solution with methyl orange (MO) dye as a model pollutant. The ZnO powder (0.1g) was added to 100 mL of dye solution. The concentration of dye was 10 mg/L. Xenon lamp (350 W) was used as a radiation (sunlight simulating) source. Samples of solution with ZnO powder have been illuminated, from 10 to 60 minutes. After illumination, they were centrifuged in order to remove catalyst. Finally, the absorption of MO dye was measured using spectrophotometer (Agilent Cary 4000).

## Results and discussion

### *FESEM view of the general mesoscopic and nanoscopic morphology of ZnO structures*

The general morphology analysed by FESEM, is shown in Fig. 1. The FESEM images clearly exhibit three different morphologies of ZnO structures, with dimensions on micro- and nano-scale, in form of prisms (a), spiky sticks (b) and grass blades (c).

The structures in Fig. 1. (a) are hexagonal prisms - it cannot be considered to be rods because of the small ratio of length and thickness. It may be noted that they bind to each other, growing in the same direction. From the histograms made from FESEM images, it is found that they have a thickness between 500 nm and 1  $\mu\text{m}$ , while their length ranges between 1 and 2 microns.

In Fig. 1. (b), rods with thickness of about 300 nm and lengths of 2  $\mu\text{m}$  can be seen. The main characteristics of these rods are slightly pointed peaks – so they are named spiky sticks. This is a form interesting for specific technological applications.

The nanostructures in Fig. 1. (c) are in the form of grass blades. The corresponding histograms show that the thickness is usually about 50 nm. The ratio of the length and thickness of these nanostructures is about 14, so they can be possibly classified as a

type of nanowires. FESEM images also indicate that they are probably porous structures.

Dimension data for ZnO structures is given later in Table 1. Obviously, the concentration reduction of the precursor also reduces the thickness of the structure, emphasizing anisotropic growth. In prolonged growth of time, the length of the structures is increased, but not the thickness (not shown here).

#### *GIXRD view of the structure and nanoscopic morphology of ZnO structures*

From XRD curves, which show the intensity dependence on the diffraction angle ( $2\theta$ ), shown in Fig. 2, the crystallographic structure of the samples was examined. All recorded diffraction peaks match with crystalline hexagonal wurtzite type structure (PDF card no. 36-1451). Only dominant diffraction peaks are shown, which correspond to (100), (002) and (101) planes of ZnO.

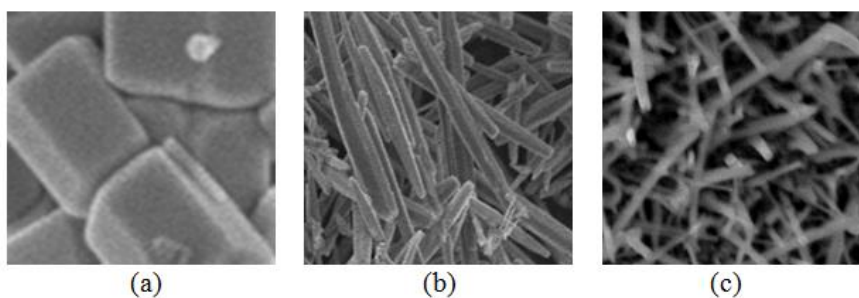


**Fig. 1.** FESEM view of ZnO structures in form of: (a) prisms (magnification: 1000x); (b) spiky sticks (magnification: 30000x); (c) grass blades (magnification: 30000x)

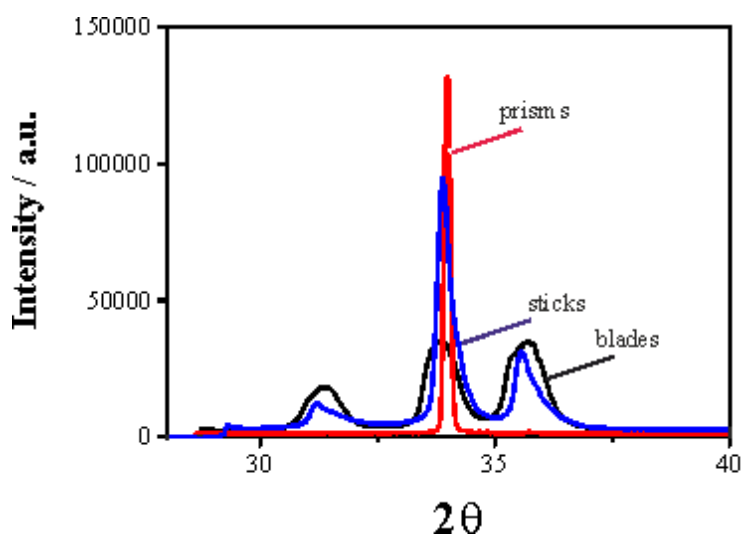


**Fig. 2.** XRD curves of ZnO structures;  $2\theta$  is the angle of diffraction

From the diffraction curves, the average monocrystalline domains - crystallites - in the ZnO structures were determined. The crystallite sizes, given in Table 1, were calculated from the profile width at half maximum height of the given peaks using the Scherrer equation (Cullity et al., 2001).

The nanometer size of crystallites showed that all ZnO structures are of polycrystalline character and can essentially be classified as nanostructured materials.

In samples with prisms and spiky sticks the (002) orientation of the crystallites is dominant, while the relative intensities of the main peaks recorded for grass blades show a randomized orientation.

These are structures in which anisotropic growth has been achieved as well as in the spiky sticks. However, only in a 0.001 M solution in which the grass blades were grown, the relatively small thickness (50 nm) on the nanoscale was achieved. Also, these structures have the smallest nanocrystallites.

As the nanoscale FESEM images indicated the possible porosity of the sample with grass blades, furthermore, we examined the morphology of the all samples by the SAXS method.

#### *SAXS view of the nanoscopic morphology*

The SAXS method shows the X-ray scattering in the sample, by measuring the dependence of the scattering intensity on the scattering angle. The presence of X-ray scattering in the area of small angles on recorded intensity maps indicates the existence of nanoheterogeneities in the density of electrons. These maps allow the specification of the dimensions of such heterogeneity - scattering object - on the nanoscale. SAXS intensity maps of ZnO samples with prisms and spiky sticks did not show the existence of nanoheterogeneities - nanoparticles or nanopores. Therefore, only the scattering in the ZnO sample with the grass blades, as shown in the map in Fig.3 was analyzed.

The analysis of the intensity map is performed in the reciprocal space, i.e. in the space of the wave vectors instead of the angles. Intensities with a

two-dimensional detector were recorded, i.e. in two directions, horizontal and vertical. These directions in the reciprocal space are represented by wave vectors  $Q_H$  and  $Q_V$ . The method of interpretation of measurement data is based on the analysis of the cuts that show the dependence of scattered intensity on these wave vectors. Intensity cuts, i.e. one-dimensional scattering curves, taken from the intensity map in Fig. 3, at fixed horizontal or vertical vector values close to the reflection plane ( $Q_H = 0$ ), are indicated by white lines. They are processed by the Guinier's analysis, commonly used to estimate the average size of the nanoheterogeneity, by calculating the average radius of the gyration (Guinier, 1939; Lavčević et al., 2007).

Calculated radii of gyration have similar values in both directions, indicating that the scattering objects are of spherical or anisotropic form with random orientation.

The resulting average diameter of about 5 nm does not match the average value of the nanocrystals in this sample (Table 1). Since nanocrystals can not be larger than nanoparticles (particles can consist of one or more nanocrystals), this result shows that scattering objects are not nanoparticles, but nanopores within the grass blades. Thus, the SAXS maps of samples with prisms and spiky sticks did not show the existence of nanoparticles or nanopores, but they showed the mesoporosity of ZnO nanostructures in the form of grass blades. So the SAXS experiment did not show the existence of nanoparticles and nanopores in prisms and spiky sticks, but clearly demonstrated the mesoporosity of grass blades.

It is expected that ZnO structures in form of grass blade, with described morphological characteristics on nanoscale, have increased number of defect states like oxygen vacancies and zinc interstitials, which can improve photocatalytic activity of ZnO, by offering a high surface area for reaction and improving the separation and transport of charges generated by irradiation. These characteristics should be taken into account even for photocatalytic activity under visible light.

**Table 1.** The average values of thickness, length and crystallite size of ZnO structures, estimated from FESEM and XRD data

Form of ZnO	Average thickness/nm	Average length/nm	Average crystallite size/nm
prisms	550	1100	100
spiky stick	300	2000	40
grass blade	50	800	15

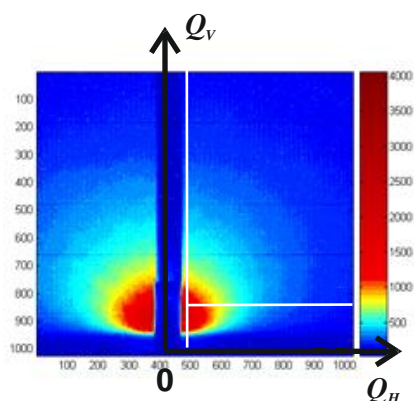


**Fig. 3.** Two-dimensional SAXS intensity maps of ZnO nanostructures in form of grass blade

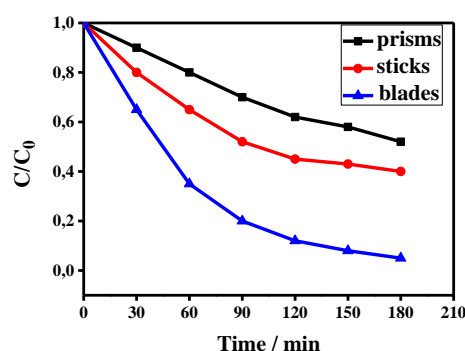


**Fig. 4.** Variation of MO concentration with exposure time.  $C_0/C$  ratio measures the percentage of degradation;  $C_0$  is the initial concentration of the dye, and  $C$  is concentration after a given time of irradiation

#### Photocatalytic activity test on Methyl Orange dye

The photocatalytic activity of ZnO nanostructures was tested in a solution with a model pollutant (Methyl Orange dye), using sun-like radiation. The absorption of dye in solution was measured after exposure during selected time intervals.

To examine the photocatalytic activity we calculated the ratio of the dye concentrations, according to the following formula (Tang et al., 1995).

$$C/C_0 = A/A_0$$

$C_0$  and  $C$  are the initial pollutant concentration and the residual concentration after irradiation time,  $A_0$  is the absorbance of pollutant before irradiation and  $A$  is the absorbance measured after a given time of irradiation. The degradation of Methyl Orange dye, proportional to the variation of concentration ratio in time, is demonstrated by Fig. 4.

It is shown that ZnO nanostructures in form of mesoporous grass blade act as efficient photocatalyst in sunlight – in their presence degradation of Methyl Orange dye takes place within approximately 180 min. The remaining two samples do not use the solar spectrum sufficiently.

#### Conclusions

In summary, samples of ZnO micro/nanostructures were prepared by hydrothermal deposition in form of prism, spiky stick and grass blade.

The precise characterization of morphology was performed by scanning electronic microscopy, XRD and SAXS methods. It is shown that the reduction of the precursors concentration reduces the thickness of the structure, emphasizing anisotropic growth. All ZnO structures are polycrystalline with nanosized crystallites. However, only ZnO structures in form of grass blade have nanosized thickness and exhibit mesoporosity.

Although all ZnO structures could be used as effective photocatalysts when exposed to UV radiation, only structures in form of grass blades have shown remarkable photocatalytic activity against a model dye pollutant in sunlike light.

The enhanced activity can be ascribed to the numerous defects and specific mesoporous morphology of those structures that enabled the enhanced absorption of radiation and efficient separation and transport of charges.

### Acknowledgement

The authors acknowledge the support of the Ministry of Science, Education and Sports of the Republic of Croatia.

### References

- Amenitsch, H., Bernstorff, S., Laggner, P. (1995): High-flux beamline for small-angle X-ray scattering at ELETTRA. *Rev. Sci. Instrum.* 66, 1624-1626. <https://doi.org/10.1063/1.1145864>
- Baruah, S, Dutta, J. (2009): Hydrothermal growth of ZnO nanostructures. *Sci. Technol. Adv. Mater.* 10, 013001 (18 pp). <https://doi.org/10.1088/1468-6996/10/1/013001>
- Baruah, S, Pal, S. K, Dutta, J. (2012): Nanostructured zinc oxide for water treatment. *Nanosci. Nanotech.– Asia* 2,90-102. <https://doi.org/10.2174/2210681211202020090>
- Colon, G., Belver, C., Fernandez-García, M. (2007): Nanostructured Oxides in Photocatalysis, in Synthesis, Properties and Applications of Solid Oxides. Rodríguez, J. A., and Ferandez-García, M. (Eds.), Wiley, New York, pp. 491-562.
- Guinier, A. (1939): La diffraction des rayons X aux très petits angles; application a l'étude de phénomènes ultramicroscopiques. *Ann. Phys.* 12, 161-237. <https://doi.org/10.1051/anphys/193911120161>
- Kumari, L., Li, W. Z., Vannoy, C. H., Leblanc, R. M., Wang, D. Z. (2010): Zinc oxide micro- and nanoparticles: synthesis, structure and optical properties. *Mater. Res. Bull.* 45, 190-196. <https://doi.org/10.1016/j.materresbull.2009.09.021>
- Langford, J. I, Wilson, A.J.C. (1978): Scherrer after Sixty Years: A Survey and Some New Results in the Determination of Crystallite Size. *J. Appl. Cryst.* 11, 102-113. <https://doi.org/10.1107/S0021889878012844>
- Lavčević, M., Turković, L. (2002): A., Small-angle X-ray scattering and wide-angle X-ray diffraction on thermally annealed nanostructured TiO<sub>2</sub> films. *Thin Solid Films* 419, 105-113. [https://doi.org/10.1016/S0040-6090\(02\)00774-5](https://doi.org/10.1016/S0040-6090(02)00774-5)
- Lavčević, M. Lučić, Dubček, P, Turković, A, Crnjak-Orel, Z, Bernstorff, S. (2007): Nanostructural depth profile of vanadium/cerium oxide film as a host for lithium ions. *Sol. Energy Mater. Sol. Cells.* 91, 616-620. <https://doi.org/10.1016/j.solmat.2006.11.013>
- Tang, Z., An, H. (1995): UV/TiO<sub>2</sub> photocatalytic oxidation of commercial dyes in aqueous solutions. *Chemosphere* 31, 4157-4170. [https://doi.org/10.1016/0045-6535\(95\)80015-D](https://doi.org/10.1016/0045-6535(95)80015-D)

---

**Received:** November 24, 2017

**Accepted:** December 6, 2017